

Detection of Eye Movements From fMRI Data

Michael S. Beauchamp*

Awake humans make eye movements with amplitudes and frequencies that depend on behavioral state and task. This poses two problems for functional magnetic resonance imaging (fMRI) studies that compare brain activity across tasks. First, motion of the eye in the orbit increases the variance of the MR signal in adjacent regions of the orbitofrontal cortex, hampering activation detection. Second, eye movements are associated with activity in a distributed network of brain areas, confounding comparisons of task activation. Direct measurement of eye movements in the scanner bore is possible with expensive and technically demanding equipment. A method is described that detects eye movements directly from MR data without the use of additional equipment. Changes in the MR time series from the vitreous of the eye were observed that correlated with eye movements, as measured directly with an infrared pupil tracking system. In each of 10 subjects, the variance of the MR time series from the eye vitreous was greater when the subject made eye movements than when the subject fixated centrally (average standard deviation (SD) 99.7 vs. 75.6, $P = 0.001$). The assessment of eye movements directly from fMRI data may be especially useful for retrospective and meta-analyses. *Magn Reson Med* 49:376–380, 2003. Published 2003 Wiley-Liss, Inc.†

Key words: electrooculography; vitreous body; neuroimaging; physiological noise; BOLD

Human subjects often make voluntary or involuntary head movements during fMRI measurements. Because even small head movements can render fMRI data unusable (1), research has focused on the development of techniques to prevent head movements (2,3), measure head movements if they occur (4,5), and correct the errors introduced by head movements (6–8).

Much less attention has been paid to the problem of eye movements in fMRI experiments. Awake humans make eye movements frequently (approximately every 250 ms) and there are at least two ways that eye movements can degrade blood oxygenation level dependent (BOLD) fMRI data. The first problem caused by eye movements is an indirect effect on the MR signal in nearby brain regions. Bulk motion, such as motion of the tongue or jaw, causes magnetic field changes in nearby tissue, resulting in image distortion and other artifacts (9). Similarly, movement of the eye in the orbit and contraction of the extraocular muscles can cause magnetic field changes in nearby brain regions. These large signal changes make it difficult to measure the small signal changes caused by BOLD activation. The second problem caused by eye movements is their effect on oculomotor control areas. When humans

make eye movements, a broadly distributed network of brain areas is active, including regions of the frontal lobe, parietal lobe, and occipital-temporal cortex (10–13). If a study aims to compare the brain activity generated by two task conditions, and the subjects make more eye movements in one condition than in the other, indirect brain activity differences due to oculomotor control will be confounded with direct differences due to the tasks themselves.

An obvious solution to these concerns is to measure eye movements. Recently, techniques have been developed that allow for measurement of eye movements in the scanner bore during imaging with high spatial and temporal resolution (14,15). However, the hardware and software needed for eye tracking are expensive and require installation in the scanner and control room. Because of the technical difficulty and expense involved, the majority of fMRI studies are conducted without in-bore eye-movement measurement.

Because of the possible confounding effects of eye movements, it would be valuable to obtain some measurement of eye movements directly from fMRI data. Human saccadic eye movements are rapid (~50 ms), and the slow TRs (~1–10 s) typically used for fMRI make it difficult to image the occurrence of individual eye movements. However, fMRI experiments usually consist of multiple brain volumes collected over 30–120 min, with subjects performing a given behavioral task for seconds or minutes at a time. We hypothesized that during a behavioral task in which subjects make eye movements, MR acquisition of the slice containing the eye should occasionally coincide with eye movements, leading to large variance in the MR signal from the eye vitreous. In contrast, when subjects do not make eye movements, variance in the MR signal from the eye should be reduced.

To test this hypothesis, we measured the standard deviation (SD) of the MR signal from the eye vitreous during two types of scan series. In one type of scan series, subjects were instructed to make eye movements to visually presented targets. In the second type of scan series, subjects viewed the same targets but were instructed to make no eye movements. An in-bore infrared pupil tracking system was used to verify the subjects' performance. Across 10 subjects, we observed significantly greater SD of the MR signal in the vitreous during eye movements than during fixation control.

METHODS

MRI Procedures

A high-resolution spoiled gradient-echo (SPGR) scan was collected in addition to six to 10 functional scan series. Each functional scan series contained volumes of 120 echo-planar images, collected using a 1.5 T scanner (General Electric, Milwaukee, WI) with repetition time

Laboratory of Brain and Cognition, National Institute of Mental Health, Bethesda, Maryland.

*Correspondence to: Michael S. Beauchamp, Ph.D., NIMH/LBC, 10 Center Drive MSC 1366, Building 10, Room 4C104, Bethesda, MD 20892-1366. E-mail: mbeauchamp@nih.gov

Received 17 June 2002; revised 5 September 2002; accepted 5 September 2002.

DOI 10.1002/mrm.10345

Published online in Wiley InterScience (www.interscience.wiley.com).

Published 2003 Wiley-Liss, Inc. † This article is a US Government work and, as such, is in the public domain in the United States of America.

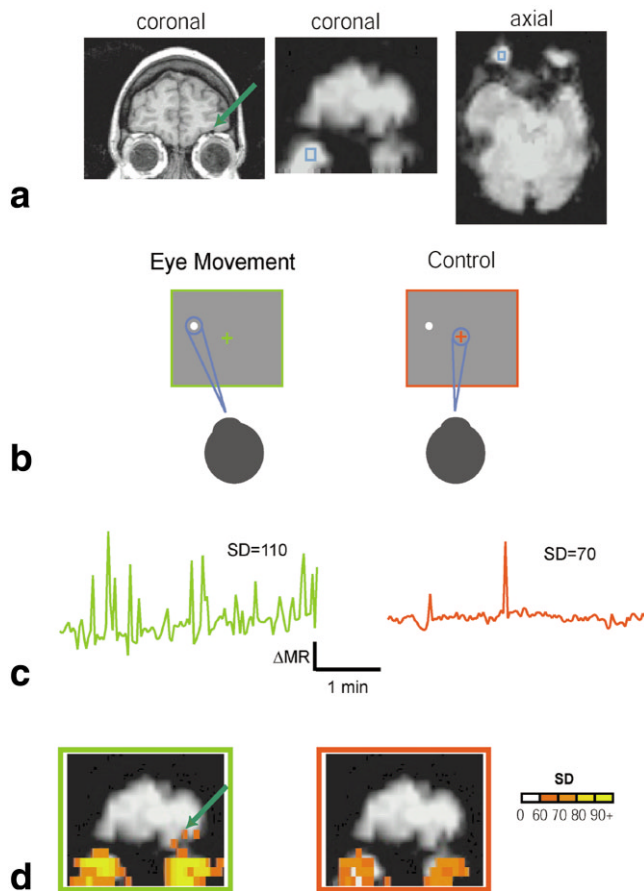


FIG. 1. **a:** Structural and functional MR images of the eye and the orbit in a single subject (case BL). Left panel: coronal slice through a 1-mm³ SPGR dataset, showing the location of the orbit, eye, and adjacent orbitofrontal cortex (dark green arrow). Eye vitreous is dark in the T_1 -weighted image. Middle panel: coregistered coronal slice through an EPI dataset (voxel size 84 mm³). Eye vitreous is bright in the T_2/T_2^* -weighted image. Right panel: axial slice through the EPI dataset. The blue box in the middle and right panels indicates the location of the voxel whose time series is shown in part **c**. **b:** Schematic illustration of visual stimulus and eye-movement task. In each 240-s scan series, subjects viewed a display in the center of which was either a green crosshair (left panel) or a red crosshair (right panel). Both displays contained moving circular targets (white dot). During the eye-movement scan series (green), the subjects moved their center-of-gaze (illustrated by blue circle) to track the moving target. During the control scan series (red), the subjects kept their eyes stationary on the fixation crosshairs. **c:** MR time series from a voxel located in the vitreous of the eye (location illustrated with the blue box in part **a**). Green line (left panel) shows a time series during a 240-s eye-movement scan series. Red line (right panel) shows a time series during a control scan series. Same scale for both graphs (vertical bar = 500 MR units). Greater SD was observed during eye-movement series compared with control scan series. **d:** Map of SD, overlaid on a coronal echo-planar image. Left panel shows SD during eye-movement scan series, right panel shows SD during control scan series. Note increased SD throughout the eye during the eye-movement scan series, and in the adjacent orbitofrontal cortex (dark green arrow).

(TR) = 2000 ms, echo time (TE) = 40 ms, L-R phase encoding, nominal flip angle = 90°, in-plane resolution = 3.75 × 3.75 mm, and 16 axial slices with a thickness of 6–8 mm (depending on the geometry of each subject’s brain) to provide coverage of the brain and eyes. The first two volumes in each series, acquired before equilibrium magnetization was reached, were discarded. The last volume in each time series was acquired with TE = 50 ms and was not used in the analysis, for an effective functional scan series length of 234 s.

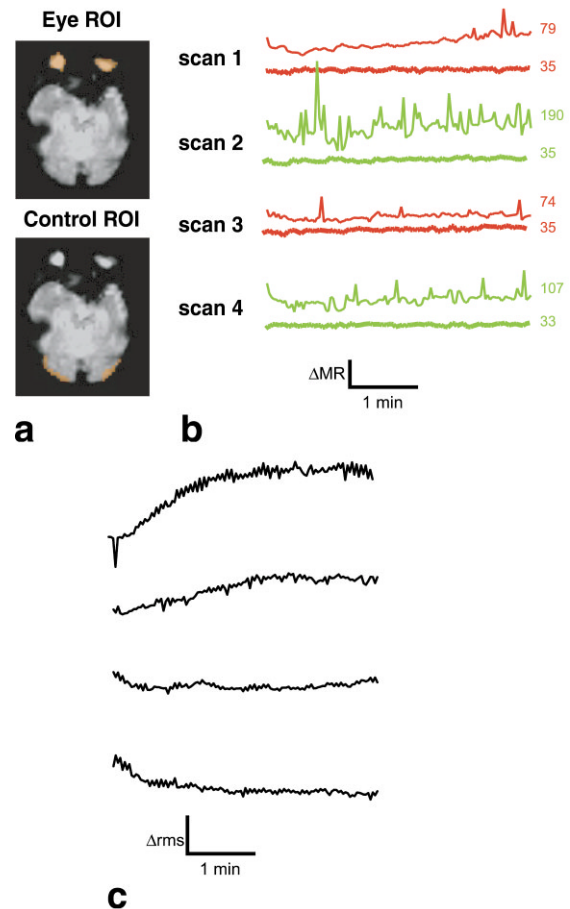


FIG. 2. Procedures for measurement of MR time series variance illustrated for a single subject (subject BL) (analysis was performed similarly for all subjects). **a:** Eye and control ROIs. An automated region-growing technique was used to label all voxels in the eye (top panel). A control ROI of the same size but distant to the eye was also created (bottom panel). A single axial slice through the eyes is shown for illustration; ROIs spanned multiple slices. Orange voxels show an ROI, overlaid on an EPI anatomical image. **b:** MR time series across conditions and ROIs. Four rows show time series for successive scan series, alternating between fixation control scan series (scans 1 and 3 in red) and eye-movement scan series (scans 2 and 4 in green). Each graph contains two traces: the top trace is the average time series from all voxels in the eye ROI; the bottom trace is the average time series from all voxels in the control ROI (ROIs illustrated in part **a**). The number at the right of each trace is the SD for that MR time series. Same scale for each graph; vertical bar is 250 MR units. **c:** Estimated magnitude of head movement vs. time for the four scan series pictured in **b**. Vertical bar is 10 RMS MR units.

Human Subjects

Ten human subjects (five males and five females, average age 29.4 years) underwent a complete physical examination and provided written informed consent in accordance with the National Institute of Mental Health (NIMH) human subjects committee. Subjects were compensated for participation in the study, and anatomical MR scans were screened by the Department of Radiology, NIH Clinical Center.

Eye Movement Task

In alternating scan series, subjects performed either an eye movement task or a control task that did not require eye movements (Fig. 1b). A small white dot was presented at varying locations in the display (116 total locations in each scan series) and subjects either moved their eyes to the location of the target each time it moved (eye movement scan series) or kept their eyes stationary at the center of the display (fixation control scan series). The subjects were instructed on which task to perform by the experimenter before each scan series. An additional cue was the color of the fixation crosshair (green for eye movements, red for fixation).

Eye Movement Acquisition and Visual Stimulus Presentation

Eye-movement data were collected using an infrared pupillary eye-tracking system (ISCAN, Inc., Burlington, MA) modified to allow operation in the MR scanner. A fiberoptic cable illuminated the subject's eye from a light source located outside the scan room. A dichroic mirror reflected visible light, allowing subjects to view a visual stimulus projected onto a screen located at the subjects' feet, while transmitting infrared wavelengths to a video camera located behind the subjects' head, outside the magnet bore. A zoom lens was used to obtain an enlarged image of the subjects' left eye. The image was then passed to a dedicated eye-movement analysis computer in the scanner control room. Horizontal and vertical eye positions were collected and calibrated using a sequence of test eye movements at the beginning and end of each session.

Region-of-Interest (ROI) Drawing

Separate eye vitreous and control ROIs were created in the subjects using AFNI software (16). A seed point was placed near the center of each eye. The vitreous of the eye has a high water content and appears bright in the T_2/T_2^* -weighted EPI images, allowing the use of a nearest-neighbor clustering algorithm to fill all voxels in each eye (stopping at a manually-selected intensity threshold of 2000). Control ROIs that met five criteria were also created in each subject: 1) the same number of voxels as the vitreous ROI, 2) located in the same axial slices as the eye ROI, 3) the same intensity threshold (>2000), 4) located on the edge of the brain, and 5) located distant from the eye in the posterior half of the brain. See Fig. 2a for vitreous and control ROIs from a single subject. The MR time series from all of the voxels in each ROI was averaged at each point in time, and the SD of the resulting time series was

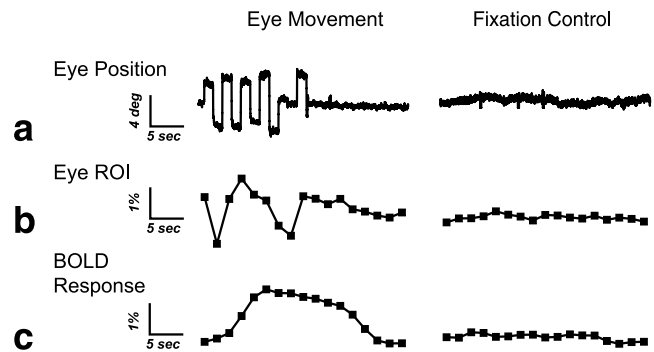


FIG. 3. Three types of data from portions of an eye-movement scan series (left column) and a fixation control scan series (right column) for a single subject (case BJ). **a:** Eye position along the horizontal axis as determined with an infrared pupil tracker. Note movements during the eye-movement scan series but not the control scan series. **b:** Average MR time series from an ROI in the eye vitreous. Rapid changes in the signal from the eye (variance increases) were observed during eye movements but not during fixation control. **c:** Average MR time series from an ROI in the occipital cortex. The BOLD signal rises after eye movements begin, and falls after eye movements cease.

then computed. This procedure was repeated for each scan series for each subject. Within each subject, an unpaired t -test was used to compare the variance of all control scan series with all eye movement scan series, and two values were calculated for the mean eye movement and control variances. A paired t -test of these values was used to calculate the significance of variance differences across subjects.

RESULTS

The vitreous of the eye was clearly delineated in the echo-planar images (Fig. 1a). During successive scan series, subjects were instructed to either make eye movements to visual targets or fixate centrally (Fig. 1b). As shown for a sample vitreous voxel (Fig. 1c), the MR time series contained greater variance during the eye-movement scan series than during the fixation control scan series. Figure 3 illustrates the likely source of this increased variance. Infrared pupil tracking demonstrated that subjects made rapid saccadic eye movements during eye movement scans but not during control scans (Fig. 3a). Occasionally, a rapid saccadic eye movement (duration ~ 50 ms) occurs at the same time as an MR acquisition of the eye ($TR = 2$ s), leading to a large change in the MR signal in the eye vitreous (Fig. 3b). Most often, the eye movement will not coincide with acquisition, resulting in a relatively stable signal within the eye. Over the course of an entire scan series, enough saccades will coincide with acquisitions to give rise to increased variance in the eye ROI (Fig. 1c, left panel) compared with control fixation scans (Fig. 1c, right panel).

To show the spatial extent of this effect, a map of SD was constructed (Fig. 1d). Variance increased throughout the vitreous during eye movement scans compared with control scans. Voxels in orbitofrontal cortex adjacent to the

Table 1
Variance of the MR Signal Across Two Conditions (eye movements and fixation) and Two ROIs (eye vitreous and control) From Ten Subjects

Subject code	Eye ROI Eye movements		Fixation		Control ROI Eye movements		Fixation	
	Mean	SEM	Mean	SEM	Mean	SEM	Mean	SEM
BH	121.5	9.7	99.4	4.0	38.4	1.5	32.9	1.2
BI	60.9	2.8	41.6	4.2	28.7	0.3	27.9	0.4
BJ	65.6	3.4	50.9	6.6	34.6	0.8	33.8	0.3
BL	142.8	24.6	76.2	3.3	33.8	0.7	34.3	0.5
BN	80.3	3.6	62.8	7.1	30.6	0.2	29.9	0.6
BO	161.0	22.6	140.0	17.8	48.9	0.9	47.2	0.3
BP	88.4	7.1	67.9	4.4	38.1	1.0	34.7	0.5
BQ	67.9	3.1	45.2	2.7	51.7	3.2	48.6	1.9
BR	130.8	6.9	100.2	4.0	32.6	0.7	32.7	0.8
BS	77.8	4.2	71.8	10.9	57.9	2.9	59.3	3.4
Average	99.7	11.4	75.6	9.6	39.5	1.2	38.1	1.0

Each row shows data for a single subject (two-letter subject code shown in leftmost column): first four columns are for the eye vitreous ROI, second four columns are for the control ROI. During each scan series, a subject performed either eye movements or fixation; the SD of the average MR time series from all of the voxels in each ROI was calculated for each scan series. The mean is the mean SD across scan series of a given type (eye movements or fixation) and the SEM is the standard error across scan series. For the average values (last row), the mean is the mean across subjects and the SEM is the standard error across subjects.

eye also showed increased variance during eye movement scans, likely due to susceptibility effects.

As shown in Fig. 2b, the average time series from the eye ROI showed increased SD in eye movement scan series compared with control scan series (average SD across three scan series of each type for this subject: 142.8 vs. 76.2, $P = 0.02$). The same effect was not observed in a control ROI located far from the eye (33.8 vs. 34.3, not significant).

A possible confounding effect for the interpretation of these observations is the occurrence of head movements. If subjects made more head movements during the eye-movement scan series than during the control scan series, increased SD in the eye ROI would be observed that would not be due to the eye movements themselves.

Several lines of evidence suggest that this is unlikely. First, subjects were instructed to keep their heads motionless in both types of runs, and a forehead strap was used to secure the subject's head to the head coil. Second, head movements typically cause a rim artifact in which voxels at the edge of the brain show high variance as the partial-volume fraction of tissue changes, causing large changes in signal intensity with even slight movements. Our control ROI was chosen to include many voxels at the edge of the brain to emphasize this effect. Even so, the control ROI showed equal variance during both types of scan series. As an additional control, the amount of head movement in each type of scan series was measured using a volume registration technique that estimated motion parameters for each time point in each scan series (8). As shown in Fig. 2c, little head motion was observed in either the eye-movement or the control scan series, and did not correlate with large signal changes in the eye ROI. There was no significant difference in estimated motion between the eye-movement and control scan series. These lines of evidence suggest that the increased SD observed in the eye ROI is due to eye movements, and not to head movements or other global causes of increased variance in the MR time series.

To determine the consistency of the effect, the same analysis was performed in 10 subjects (Table 1). In every subject, greater variance was observed within the eye ROI for eye movements compared with fixation control (average variance across subjects 99.7 vs. 75.6, $P = 0.001$). In contrast, the control ROI did not show a difference between conditions.

The effects of eye movements are twofold. First, in the eye and neighboring brain regions (Fig. 1d), variance increases whenever an eye movement coincides with an MR acquisition of the eye (Fig. 3b). Second, in a broad network of brain regions, neural activity related to the eye movement causes a BOLD increase in the MR time series (Fig. 3c). This indirect change due to the BOLD response (slow rise and fall in the mean MR signal) is markedly different from the direct change caused by eye movements (no change in mean signal, increased variance).

DISCUSSION

These results show that it is possible to detect the occurrence of eye movements directly from MR data using imaging parameters commonly used for BOLD-EPI fMRI. The relatively slow TR (2 s) means that eye-movement measurement is a random process: if an eye movement happens to occur during a slice acquisition containing the eye, the MR signal from the eye vitreous at that time point will differ from baseline (Fig. 3). While on average a task with more eye movements will result in increased variance in the signal from the vitreous (Table 1), the amount of variance increase will differ from scan series to scan series (Fig. 2b, Table 1). This means that individual eye movements cannot be detected, and that averaging across a number of scan series is necessary to estimate eye movement differences between tasks. However, this is not an undue limitation for fMRI studies, which typically require a number of scan series to produce accurate activation maps. In the present study, eye-movement conditions and

fixation control conditions were in consecutive scan series; however, this technique should also be applicable to other types of experimental designs in which different task conditions are more closely spaced in time.

Clearly, examination of vitreous variance will not replace dedicated hardware that allows the measurement of eye movements with great spatial and temporal precision. However, because most fMRI experiments are performed without in-bore eye tracking, a simple (albeit imprecise) measurement of eye movements from MR data alone is useful. First, as shown in Fig. 1d, eye movements can increase the MR signal variance in voxels near the eye, including the orbitofrontal cortex. Therefore, fMRI studies that expect to see activation in this region (implicated in emotion and emotion-related learning (17)) would be well advised to measure vitreous variance to ensure that it is not masking orbitofrontal activation. Second, this technique may be valuable for meta-analyses or retrospective studies. A number of large-scale efforts are under way to create databases (e.g., at the Functional Magnetic Resonance Imaging Data Center) containing vast numbers of fMRI datasets collected from investigators worldwide (18). The collected data is then distributed to other investigators for post hoc analysis. A study in the database might have two task conditions (such as viewing pictures of tools and pictures of humans (19)) and report task activation differences in regions of frontal, parietal, or occipital lobes that overlap with eye-movement control areas. An analysis of vitreous variance might allow an approximate answer to the question of whether these activation differences are due to the pictures themselves or to eye-movement differences between the two tasks.

The most important requirement for the method described here is that the fMRI acquisition volume must include at least one slice through the eye vitreous. The more rapid the TR (and the more slices that include the vitreous), the more likely that an eye movement will coincide with an eye acquisition. Therefore, the 2-s TR used here, or a faster one, may be necessary for accurate eye-movement comparisons to be made between tasks.

ACKNOWLEDGMENTS

The author thanks Robert Cox and Rasmus Birn for helpful comments on the manuscript, and Giorgio Ganis for discussion.

REFERENCES

1. Field AS, Yen YF, Burdette JH, Elster AD. False cerebral activation on BOLD functional MR images: study of low-amplitude motion weakly correlated to stimulus. *Am J Neuroradiol* 2000;21:1388–1396.
2. Thulborn KR, Shen GX. An integrated head immobilization system and high-performance RF coil for fMRI of visual paradigms at 1.5 T. *J Magn Reson* 1999;139:26–34.
3. Fitzsimmons JR, Scott JD, Peterson DM, Wolverton BL, Webster CS, Lang PJ. Integrated RF coil with stabilization for fMRI human cortex. *Magn Reson Med* 1997;38:15–18.
4. Enzmann DR, Pelc NJ. Brain motion: measurement with phase-contrast MR imaging. *Radiology* 1992;185:653–660.
5. Seto E, Sela G, McIlroy WE, Black SE, Staines WR, Bronskill MJ, McIntosh AR, Graham SJ. Quantifying head motion associated with motor tasks used in fMRI. *Neuroimage* 2001;14:284–297.
6. Ashburner J, Andersson JL, Friston KJ. High-dimensional image registration using symmetric priors. *Neuroimage* 1999;9(6 Pt 1):619–628.
7. Friston KJ, Williams S, Howard R, Frackowiak RS, Turner R. Movement-related effects in fMRI time-series. *Magn Reson Med* 1996;35:346–355.
8. Cox RW, Jesmanowicz A. Real-time 3D image registration for functional MRI. *Magn Reson Med* 1999;42:1014–1018.
9. Birn RM, Bandettini PA, Cox RW, Jesmanowicz A, Shaker R. Magnetic field changes in the human brain due to swallowing or speaking. *Magn Reson Med* 1998;40:55–60.
10. Beauchamp MS, Petit L, Ellmore TM, Ingeholm J, Haxby JV. A parametric fMRI study of overt and covert shifts of visuospatial attention. *Neuroimage* 2001;14:310–321.
11. Corbetta M, Akbudak E, Conturo TE, Snyder AZ, Ollinger JM, Drury HA, Linenweber MR, Petersen SE, Raichle ME, Van Essen DC, Shulman GL. A common network of functional areas for attention and eye movements. *Neuron* 1998;21:761–773.
12. Nobre AC, Gitelman DR, Dias EC, Mesulam MM. Covert visual spatial orienting and saccades: overlapping neural systems. *Neuroimage* 2000;11:210–216.
13. Kimmig H, Greenlee MW, Gondan M, Schira M, Kassubek J, Mergner T. Relationship between saccadic eye movements and cortical activity as measured by fMRI: quantitative and qualitative aspects. *Exp Brain Res* 2001;141:184–194.
14. Gitelman DR, Parrish TB, LaBar KS, Mesulam MM. Real-time monitoring of eye movements using infrared video-oculography during functional magnetic resonance imaging of the frontal eye fields. *Neuroimage* 2000;11:58–65.
15. Kimmig H, Greenlee MW, Hueth F, Mergner T. MR-eyetracker: a new method for eye movement recording in functional magnetic resonance imaging. *Exp Brain Res* 1999;126:443–449.
16. Cox RW. AFNI: software for analysis and visualization of functional magnetic resonance neuroimages. *Comput Biomed Res* 1996;29:162–173.
17. O'Doherty J, Kringelbach ML, Rolls ET, Hornak J, Andrews C. Abstract reward and punishment representations in the human orbitofrontal cortex. *Nat Neurosci* 2001;4:95–102.
18. Van Horn JD, Grethe JS, Kostelec P, Woodward JB, Aslam JA, Rus D, Rockmore D, Gazzaniga MS. The functional magnetic resonance imaging data center (fMRIDC): the challenges and rewards of large-scale databasing of neuroimaging studies. *Phil Trans R Soc Lond B Biol Sci* 2001;356:1323–1339.
19. Beauchamp MS, Lee KE, Haxby JV, Martin A. Parallel visual motion processing streams for manipulable objects and human movements. *Neuron* 2002;34:149–159.